ADVANCED MATERIALS TECHNOLOGIES
www.advmattechnol.de

Formation of Semiconducting Supramolecular Fullerene Aggregates in a Dipeptide Organogel

*Priyadarshi Chakraborty, Wei Ji, Stav Rahmany, Lioz Etgar, and Ehud Gazit**

The formation of nanostructured fullerene aggregate inside supramolecular gels is a topic of great interest because of the potential applications of these nanostructures in photoelectronics. Gel phase facilitates the aggregation of fullerene by restricting the movement of solvent molecules, thereby increasing the local fullerene concentration. Herein, the supramolecular nanostructure formation of fullerene (C_{60}) in a minimalistic dipeptide (diphenylalanine, FF) organogel is reported. The resulting composite FF/Fullerene gels exhibit improved mechanical properties and semiconductivity. While fullerene nanostructures do not disturb the FF aggregation pattern, they adhere to the FF fibers via non-covalent interaction. Morphological analysis reveals the presence of spherical clusters and nanorods of fullerene attached to the dipeptide fibers. The composite gel with highest fullerene concentration exhibits linear current–voltage response with a current magnitude of ≈0.3 nA. Moreover, poly(3,4-ethylenedioxythiophene):polystyrene sulfonate (PEDOT:PSS) is incorporated in the FF/Fullerene system yielding tri-hybrid donor–acceptor gels which exhibit photoresponsive conductivity. Therefore, the FF/Fullerene and the tri-hybrid gel have interesting properties, and holds significant promise toward photoelectronic device applications.

Short-peptide self-assembly has attracted immense research interest due to their intriguing properties and manifold applications.[1–9] Supramolecular gels are a product of self-assembly process where aggregated fibers entangle within themselves forming a 3D network structure.[10–12] Short-peptide based supramolecular hydrogels are excellent candidates for biomedical applications due to their intrinsic biocompatibility and extra cellular matrix mimicking attributes.[13–15] Recently, peptide-based hybrid hydrogels were also developed from our research group in order to improve the mechanical property of the native hydrogels, as well as to confer conductivity.[16,17] Although short-peptides have been meticulously studied as hydrogelators,[18] their organogelation ability is rarely reported in literature. One exception being diphenylalanine (FF), which was reported to exhibit gelation behavior in toluene or chloroform.[19–23] FF is the simplest aromatic dipeptide made of natural amino acids, and the core recognition motif of Aβ polypeptide. Our research group first demonstrated the self-assembling ability and nanotube formation of FF from its aqueous solution.[6] These nanostructures also served as a template for preparing Ag nanowires. FF organogels are intriguing as well, due to their transformation into microcrystals by simple cryogenic treatment.[22] Moreover, these FF organogels were also capable of immobilizing inorganic quantum dots demonstrating them to be excellent soft templates.[19]

Fullerene (C_{60}) is a zero dimensional carbon based material which is very important because of its semiconducting properties and potential applications in photoelectronic field.[24–26] Fullerene is an electron-acceptor, and its composite with electron rich molecules create donor–acceptor heterojunctions which play a crucial role in organic electronic devices.[27–30] Fullerenes exhibit different aggregation patterns in different donor medium and experimental conditions, resulting in diverse nanostructures while retaining their optoeletronic properties.[31–35] Therefore, there is an increasing trend amongst material scientists to discover de novo hybrids of fullerenes and π-conjugated systems.[36–40] As fullerenes exhibit affinity toward gelators with aromatic groups or π-conjugation,[41] many researchers have demonstrated the interactions between supramolecular π-gels and fullerene.[28,42–46] Ajayaghosh and co-workers reported the crystallization of fullerene (C_{60}) to supramolecular rods with increased photoconductivity in a oligo(*p*-phenylenevinylene) based organogel.[47] Very recently, Fang and co-workers reported the growth of long crystalline fullerene (C_{60}) fibers in supramolecular gels using an anti-solvent approach. The device fabricated from these crystalline fibers exhibited high-performance photodetection.[48] Therefore, the aggregation of fullerene in supramolecular gels is a topic of great interest when viewed from the perspective of photoelectronic applications.

Dr. P. Chakraborty, Dr. W. Ji, Prof. E. Gazit
School of Molecular Cell Biology and Biotechnology
George S. Wise Faculty of Life Sciences
Tel Aviv University
Tel Aviv 6997801, Israel
E-mail: ehudg@post.tau.ac.il

S. Rahmany, Prof. L. Etgar
Institute of Chemistry
Casali Center for Applied Chemistry
The Hebrew University of Jerusalem
Jerusalem 91904, Israel

Prof. E. Gazit
Department of Materials Science and Engineering
Iby and Aladar Fleischman Faculty of Engineering
Tel Aviv University
Tel Aviv 6997801, Israel

The ORCID identification number(s) for the author(s) of this article can be found under https://doi.org/10.1002/admt.201900829.

DOI: 10.1002/admt.201900829

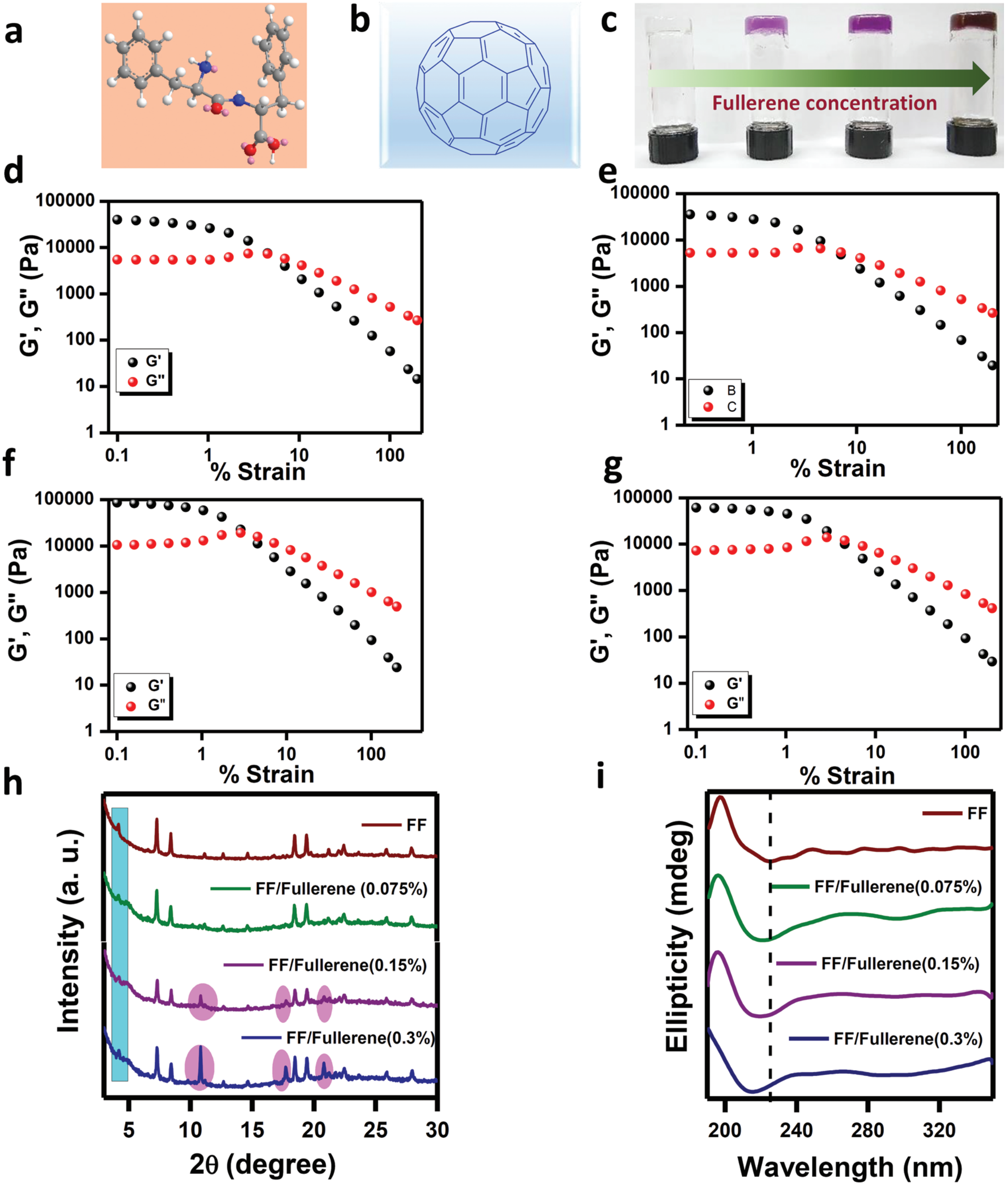

Figure 1. Representative structures of a) FF and b) fullerene. c) Digital image of the gels. Strain sweep experiments carried out on the d) FF, e) FF/Fullerene (0.075%), f) FF/Fullerene (0.15%), and g) FF/Fullerene (0.3%) gels. h) Powder XRD patterns of the dried gels. i) CD spectra of the gels.

Herein, we report a dipeptide-based organogel enabling the formation of supramolecular aggregates of fullerene inside its self-assembled networks. We selected FF dipeptide (**Figure 1**a) because of its minimal nature, excellent gelation, templating capabilities, and propensity to stack with fullerene (C_{60}) (Figure 1b) using its aromatic groups. The FF and FF/Fullerene composite gels (Figure 1c) were prepared using a solvent-switch method. FF was dissolved in 1,1,1,3,3,3-hexafluoro-2-propanol (HFP) and diluted with toluene to a final concentration of 0.5 wt%. The FF/Fullerene gels contained different concentrations of fullerene (0.075, 0.15, and 0.3 wt%) while the FF concentration was kept constant (0.5 wt%). The FF/Fullerene gels are designated as FF/Fullerene (*x*%), where *x* denotes the concentration of fullerene (wt%).

Rheological studies were performed to investigate the mechanical property of the FF and FF/Fullerene hybrid gels.[49] Strain sweep experiments (Figure 1d–g) exhibited linear viscoelastic regime (LVR) until ≈1% strain for the FF and FF/Fullerene gels. Next, we carried out frequency sweep experiments on the gels at 0.1% strain (within the LVR) (Figure S1, Supporting Information). Although, storage(G') and loss (G'') modulus values increased in the FF/Fullerene (0.15%) and FF/Fullerene (0.3%) gels, the FF/Fullerene (0.075%) gel exhibited almost similar values compared to FF gels (Table S1, Supporting Information). The highest G' and G'' values were obtained in the FF/Fullerene (0.15%) gel. The G'/G'' ratio which indicates the robustness was also observed to be highest in FF/Fullerene (0.15%) gel. Both of these results indicate the FF/Fullerene (0.15%) gel to be of the highest rigidity.

In order to understand the structure of the gels, we opted for powder XRD experiments (Figure 1h). FF gel exhibited a lamellar structure with a lamellar thickness of d = 20.9 Å (2θ = 4.2°), along with some weak crystalline peaks probably arising because of the small crystallites produced during the drying process.[22] These peaks were retained in the FF/Fullerene gels indicating that fullerene does not significantly alter the packing of FF. However, some new peaks had arisen in the FF/Fullerene (0.15%) diffractogram, which sharpened in FF/Fullerene (0.3%) gels. These peaks correspond to the d spacing of 8.4, 5, and 4.2 Å (2θ = 10.8°, 17.8°, and 20.8° respectively). The appearance of these peaks surmises the formation of rod-like aggregates of fullerene inside the gel network.[47]

CD spectra of FF gel (Figure 1i) exhibited a negative Cotton effect at 226 nm signifying predominant β-sheet arrangement of the FF molecules.[19] Evidently, this β-sheet arrangement remained intact for the FF/Fullerene gels although, a blue shift in the band was observed. This signifies that while fullerene does not affect the internal packing arrangement of the gel, it

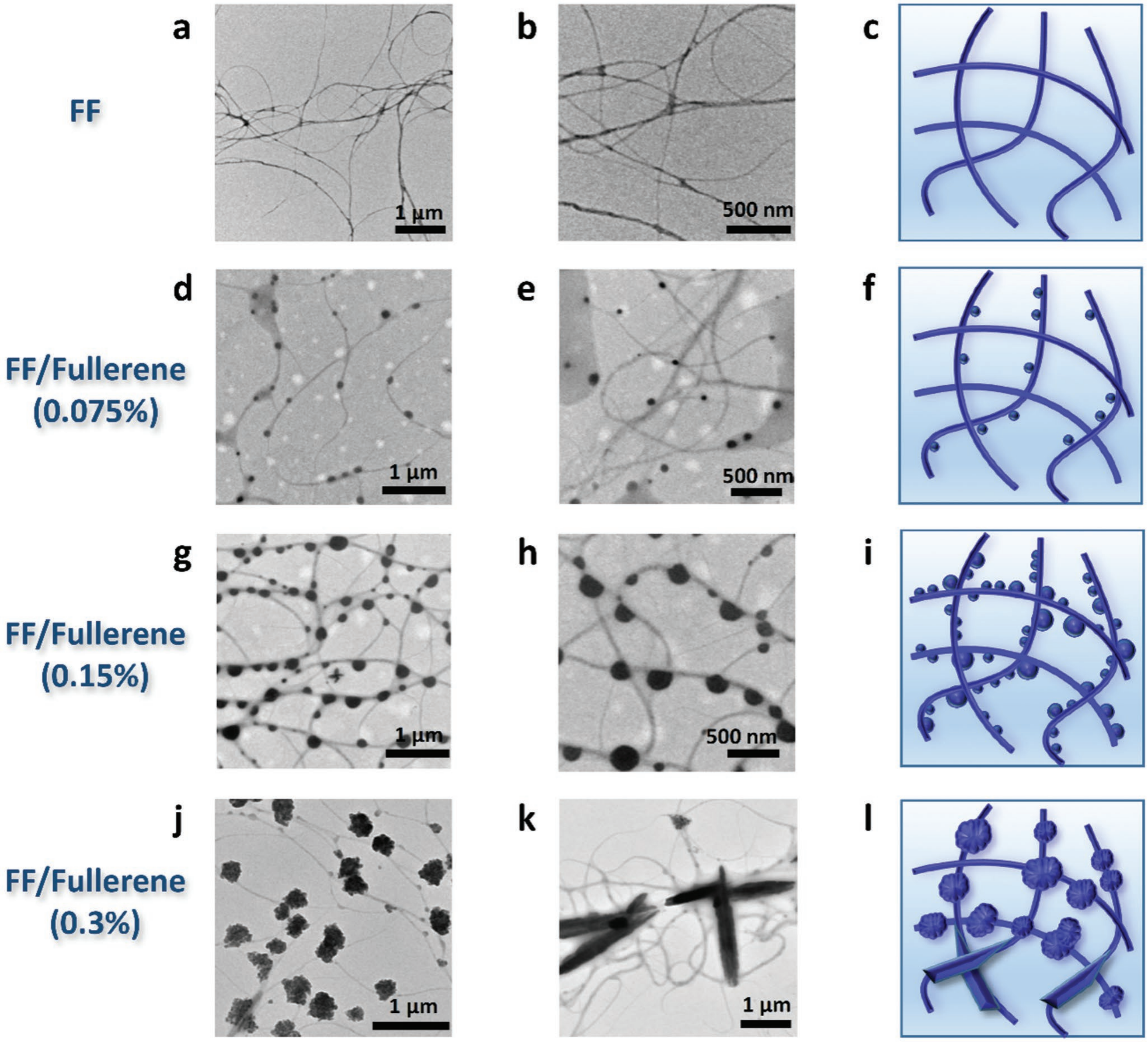

Figure 2. TEM micrographs and schematic representation of the nanostructures of a–c) FF, d–f) FF/Fullerene (0.075%), g–i) FF/Fullerene (0.15%), and j–l) FF/Fullerene (0.3%) gels.

might interact with FF nanostructures via non-covalent interactions. This assumption is also supported from the FTIR spectra (Figure S2, Supporting Information) where the peaks representing the β-sheet arrangement in the FF gel (1687 and 1610 cm^{-1})[19] remained unchanged after addition of fullerene.

UV–vis absorption spectra of the dried FF and FF/Fullerene gels are presented in Figure S3, Supporting Information. After addition of 0.075% fullerene to the FF gels, an absorption peak at ≈450 nm emerged (Figure S3b, Supporting Information) which could be ascribed to the states resulting from exciton coupling of the UV bands.[50] In the FF/Fullerene (0.15%) gels (Figure S3c, Supporting Information) this peak blue shifted to 438 nm. The blue shift in the peak with increasing fullerene concentration may indicate its π-interaction with FF. At the highest fullerene concentration (0.3%), only a broad band between 480 and 660 nm was observed which may occur due to strong intermolecular interactions among fullerene molecules.[50]

Fluorescence spectra of FF gel (Figure S4a, Supporting Information) exhibited an emission peak at 293 nm indicating aggregation of FF molecules.[22] However, the emission almost entirely quenched after adding 0.075 wt% fullerene to the FF gels. In order to observe the FF emission peak after fullerene addition, we integrated lower concentrations of fullerene (0.0125, 0.025, and 0.03 wt%) to the FF gels (Figure S4b, Supporting Information). The emission peak of FF red shifted with increase in fullerene concentration with a quenching in the intensity, indicating π-interaction of FF with fullerene. Therefore the UV–vis absorption and fluorescence spectra suggest the signature of π-interactions between FF and fullerene.

Next, we performed transmission electron microscopy to analyze the morphology of the FF and FF/Fullerene gels (**Figure 2**). FF exhibited fibrillar network morphology with long entangled fibers (Figure 2a–c). Addition of different concentrations of fullerene to the FF gels produced clusters and nanorods of fullerene, while FF fibers remained intact. At a fullerene concentration of 0.075 wt%, spherical clusters were observed (Figure 2d–f). Interestingly, these spherical clusters were attached to the FF fibers probably due to the existence of non-covalent interactions among themselves. Further increase in fullerene concentration (0.15 wt%) caused the spherical clusters to increase in size and density (Figure 2g–i). At the highest fullerene concentration (0.3 wt%) nanorods of fullerenes were observed along with the spherical clusters (Figure 2j–l). The nanorods had a length of ≈2.5 µm and a width of ≈300 nm. High concentration of fullerene initially produces spherical clusters which subsequently nucleate to generate supramolecular nanorods.[47] This process is facilitated by the immobilization of the solvent in the gel medium which enhances the local concentration of fullerene, thus allowing the 1D growth required for producing supramolecular rods.

Next, we studied the effect of fullerene nanostructures on current–voltage (*I*–*V*) properties of the dried gels (**Figure 3**).

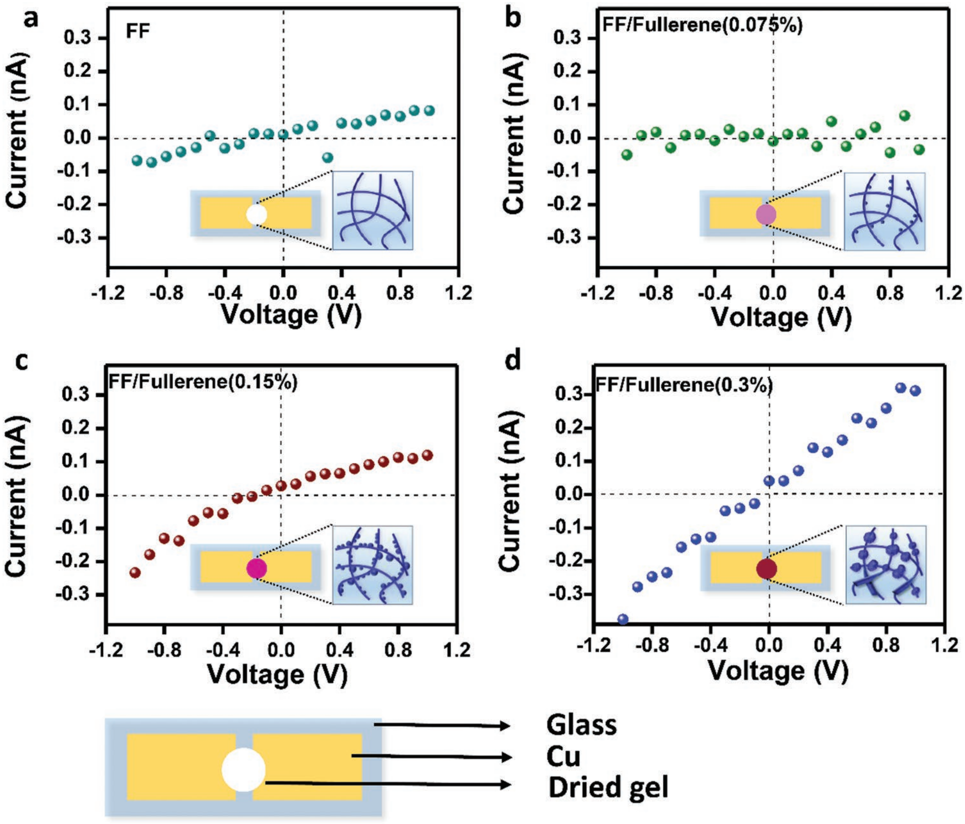

Figure 3. *I*–*V* response of the dried gels of a) FF, b) FF/Fullerene (0.075%), c) FF/Fullerene (0.15%), and d) FF/Fullerene (0.3%). The inset of each figure represents the fullerene nanostructures responsible for the observed *I*–*V* response of the corresponding gels. (Bottom: A representative diagram of the electrode used for *I*–*V* measurements).

As evident from Figure 3a,b, FF and FF/Fullerene (0.075%) dried gels failed to show any *I*–*V* response. However, at increased fullerene concentration (0.15%) an *I*–*V* response was observed with a current magnitude of ≈0.1 nA (Figure 3c). The FF/Fullerene (0.3%) gel exhibited a current of ≈0.3 nA and an almost linear *I*–*V* response (Figure 3d). Therefore, it is evident that the underlying mechanism of conduction is linked to the supramolecular nanostructures formed within the gels. With increase in fullerene concentration the size of the spherical fullerene domains increases. These spherical domains help in conducting electricity. At the highest fullerene concentration, the supramolecular fullerene nanorods facilitate the flow of current causing a linear *I*–*V* response.

In order to demonstrate an application of the newly developed FF/Fullerene composite gels, we prepared tri-hybrid systems composed of FF, fullerene, and a conductive polymer, poly(3,4-ethylenedioxythiophene):polystyrene sulfonate (PEDOT:PSS). In the tri-hybrid system, fullerene acts as an acceptor, while PEDOT:PSS plays the role of donor (**Figure** 4a,b). Self-assembled 3D networks of FF enable homogeneous dispersion of the donor–acceptor moieties inside the gel, resulting in their intimate coexistence. The *I*–*V* plot of the dried tri-hybrid gel exhibited rectification property (Figure 4c) where the rectification ratio (the ratio of current at the selected reverse bias voltage to the current at the same forward bias voltage)[51] was calculated to be ≈1.4. The formation of donor–acceptor junctions facilitated by the intimate coexistence of fullerene (acceptor) and PEDOT:PSS (donor) in the entangled self-assembled nanostructure of FF, led to the rectification property of the tri-hybrid gel.

Furthermore, the presence of donor–acceptor junctions in the tri-hybrid gel inspired us to investigate its photoresponsive conductivity. We performed *I*–*V* measurements on the dried tri-hybrid gels both in presence and absence of light, using a simple device as shown in Figure 4d. The *I*–*V* results exhibited an increase in current both in forward and reverse bias at each applied voltage, for irradiation with a constant light intensity (100 mW cm^{-2}). However, the final increment in current (at an applied voltage of 2 V) at the forward bias, was higher compared to that of the reverse bias (−2 V) (Figure 4f). This result hints at further potential utilization of the tri-hybrid system as active materials for dye-sensitized solar cells.[51]

In summary, we developed hybrid gels of the minimalistic aromatic FF dipeptide and fullerene. FF/Fullerene gels notably exhibited improved mechanical properties compared to the FF gels. Spectroscopic studies revealed the signature of β-sheet arrangements in the FF nanostructured gels which were unaffected after the addition of fullerene. However, shift in fluorescence emission maxima indicated the involvement of non-covalent interaction between FF and fullerene. FF gel was comprised of entangled fibers, whereas the FF/Fullerene gels exhibited spherical domains and nanorods of fullerene adhered to the FF fibers. The FF/Fullerene (0.3%) gels exhibited a linear

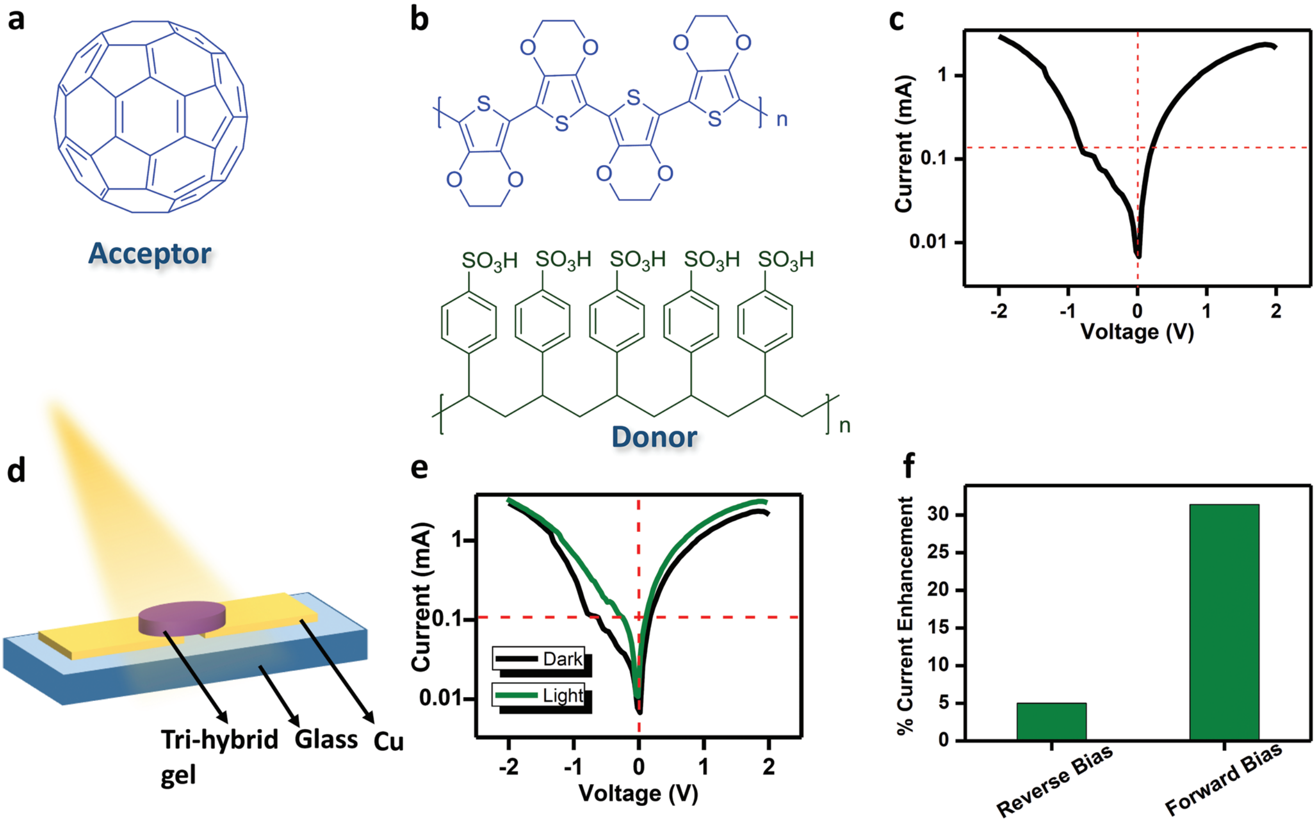

Figure 4. Photoresponsive conductivity of the tri-hybrid gels. a,b) Representative chemical structures of the acceptor (Fullerene) and donor (PEDOT:PSS) moieties as components of the tri-hybrid gel. c) *I*–*V* response of the dried tri-hybrid gel. d) A representative diagram of the simple device fabricated to measure the photocurrent response of the tri-hybrid gel. e) *I*–*V* response of the tri-hybrid gel under dark and illumination conditions. f) % Current enhancement of the tri-hybrid gel in forward and reverse bias at applied voltages of 2 and −2 V, respectively.

I–V response with a current of ≈0.3 nA, thus behaving like a semiconductor. In order to engineer a donor–acceptor system, PEDOT:PSS was incorporated in the FF/Fullerene system yielding tri-hybrid gels which exhibited photoresponsive conductivity. Therefore, the FF/Fullerene gels and the tri-hybrid gels are intriguing from the perspective of morphology and electrical properties, and promise potential applications in photoelectronics.

Experimental Section

Materials: FF was purchased from Bachem at a purity level of >98%. Fullerene (C_{60}) was procured from Holland Moran, Israel. HFP was purchased from Sigma, and toluene was purchased from Bio-Lab Ltd., Israel.

Preparation of Gels: FF was first dissolved in HFP at a concentration of 12.5 wt%. To prepare FF gels, this stock solution of FF in HFP was diluted with toluene where a final FF concentration was 0.5 wt%. Fullerene (C_{60}) was dissolved in toluene at concentrations of 0.3, 0.15, and 0.075 wt%. The respective fullerene solutions in toluene were then used to dilute the FF stock solution for the preparation of the FF/Fullerene gels. The tri-hybrid gels were prepared in a similar procedure. Briefly, 200 µL of PEDOT:PSS solution (3.0–4.0% in H_2O, high conductivity grade, Sigma-Aldrich) was dispersed in 2 mL of fullerene solution (0.3%) which was then used to dilute the FF stock solution yielding the tri-hybrid gels.

Mechanical Properties: The mechanical properties of the gels were measured on an ARES-G2 rheometer (TA Instruments, New Castle, DE, USA) using a 8 mm parallel-plate geometry with a gap of 1000 µm. 1-day aged gels were used for the measurements. Strain sweep experiments were carried out at a constant frequency of 1 Hz. Dynamic frequency sweep experiments were carried out at a constant strain of 0.1%.

Wide Angle X-Ray Scattering: Wide angle X-ray scattering patterns of the dried gels were recorded by using a Bruker d8 Advance Diffractometer equipped with Goebel mirrors to parallelize the beam and LYNXEYE XE linear detector.

CD Spectroscopy: CD and absorption spectra of all the samples were collected on an Applied Photophysics Chirascan Spectrometer with bandwidth of 1.0 using a 0.1 mm quartz cuvette.

Fourier-Transform Infrared Spectroscopy: 30 µL of the gels were deposited onto disposable KBr infrared sample cards (Sigma-Aldrich, Rehovot, Israel), and allowed to dry. The measurements were carried out in a nitrogen purged Nexus 470 FTIR spectrometer (Nicolet, Offenbach, Germany) equipped with a deuterated triglycine sulfate (DTGS) detector.

Fluorescence Spectroscopy: Fluorescence spectra of the gels were recorded using a Horiba fluoromax 4 instrument. The gels were prepared in quartz cells of 1 cm path length and excited at 280 nm. Emission scans were recorded using 3 nm excitation and emission slits.

Transmission Electron Microscopy: The gel samples were prepared according to the procedure described earlier. 10 µL of the diluted gel solutions were drop casted onto 400-mesh copper grids covered by a carbon-stabilized Formvar film (SPI, West Chester, PA, USA). The samples were dried under ambient conditions and the micrographs were recorded using a JEM-1400Plus Transmission Electron Microscope operating at 80 kV.

Conductivity Analysis: The gels were drop-casted on copper electrodes with an electrode gap of 2 mm and dried under ambient conditions. Current–voltage (*I–V*) measurements were performed on a Keithley 2450 source-meter using the two-probe method. All measurements were carried out from −1 to 1 V with 0.1 V steps. The measurements were repeated with at least three independent samples to ensure reproducibility.

Photocurrent Measurement: Photocurrent measurements were obtained using a Newport solar simulator system consisting of an Oriel *I–V* test station with an Oriel Sol3A simulator. The solar simulator was Class AAA for spectral performance, uniformity of irradiance, and temporal stability. It was equipped with a 450 W xenon lamp. The output power was adjusted to match AM1.5 global sunlight (100 mW cm^{-2}). *I–V* curves were obtained by applying a varying external bias to the device and measuring the generated photocurrent with a Keithley model 2400 digital source meter. All measurements were carried out under ambient conditions in air (temperature of 25 ± 3 °C and humidity 40% ± 10%).

Supporting Information

Supporting Information is available from the Wiley Online Library or from the author.

Acknowledgements

This work was partially supported by grants from the European Research Council under the European Union's Horizon 2020 research and innovation program (BISON, Advanced ERC grant, no. 694426) (E.G.). P.C. gratefully acknowledges Tel Aviv University for financial support and thanks the members of the Gazit laboratory for helpful discussions. The authors thank Kian Kadan-Jamal and Prof. Yosi Shacham, Department of Physical Electronics, School of Electrical Engineering, Tel Aviv University, for the help in *I–V* measurements.

Conflict of Interest

The authors declare no conflict of interest.

Keywords

diphenylalanine, fullerene, rheology, semiconductivity, short peptides

Received: September 20, 2019
Revised: December 12, 2019

---

[1] X. Yan, P. Zhu, J. Li, *Chem. Soc. Rev.* **2010**, *39*, 1877.
[2] Y. Tian, H. Wang, Y. Liu, L. Mao, W. Chen, Z. Zhu, W. Liu, W. Zheng, Y. Zhao, D. Kong, Z. Yang, W. Zhang, Y. Shao, X. Jiang, *Nano Lett.* **2014**, *14*, 1439.
[3] L. Adler-Abramovich, D. Aronov, P. Beker, M. Yevnin, S. Stempler, L. Buzhansky, G. Rosenman, E. Gazit, *Nat. Nanotechnol.* **2009**, *4*, 849.
[4] S. Bera, S. Mondal, B. Xue, L. J. W. Shimon, Y. Cao, E. Gazit, *Nat. Mater.* **2019**, *18*, 503.
[5] A. Mahler, M. Reches, M. Rechter, S. Cohen, E. Gazit, *Adv. Mater.* **2006**, *18*, 1365.
[6] M. Reches, E. Gazit, *Science* **2003**, *300*, 625.
[7] K. Tao, P. Makam, R. Aizen, E. Gazit, *Science* **2017**, *358*, eaam9756.
[8] B. Adhikari, G. Palui, A. Banerjee, *Soft Matter* **2009**, *5*, 3452.
[9] B. Adhikari, A. Banerjee, *Soft Matter* **2011**, *7*, 9259.
[10] P. Chakraborty, B. Roy, P. Bairi, A. K. Nandi, *J. Mater. Chem.* **2012**, *22*, 20291.
[11] P. Chakraborty, S. Das, S. Mondal, P. Bairi, A. K. Nandi, *Langmuir* **2016**, *32*, 1871.
[12] P. Chakraborty, S. Mondal, S. Khara, P. Bairi, A. K. Nandi, *J. Phys. Chem. B* **2015**, *119*, 5933.
[13] R. M. Gouveia, R. R. Jones, I. W. Hamley, C. J. Connon, *Biomater. Sci.* **2014**, *2*, 1222.

[14] M. Zhou, A. M. Smith, A. K. Das, N. W. Hodson, R. F. Collins, R. V. Ulijn, J. E. Gough, *Biomaterials* **2009**, *30*, 2523.
[15] V. Castelletto, C. M. Moulton, G. Cheng, I. W. Hamley, M. R. Hicks, A. Rodger, D. E. López-Pérez, G. Revilla-López, C. Alemán, *Soft Matter* **2011**, *7*, 11405.
[16] P. Chakraborty, T. Guterman, N. Adadi, M. Yadid, T. Brosh, L. Adler-Abramovich, T. Dvir, E. Gazit, *ACS Nano* **2019**, *13*, 163.
[17] P. Chakraborty, M. Ghosh, L. Schnaider, N. Adadi, W. Ji, D. Bychenko, T. Dvir, L. Adler-Abramovich, E. Gazit, *Macromol. Rapid Commun.* **2019**, *40*, 1900175.
[18] A. Dasgupta, J. H. Mondal, D. Das, *RSC Adv.* **2013**, *3*, 9117.
[19] X. Yan, Y. Cui, Q. He, K. Wang, J. Li, *Chem. Mater.* **2008**, *20*, 1522.
[20] P. Zhu, X. Yan, Y. Su, Y. Yang, J. Li, *Chem. - Eur. J.* **2010**, *16*, 3176.
[21] H. L. Sun, Y. Chen, X. Han, Y. Liu, *Angew. Chem., Int. Ed.* **2017**, *56*, 7062.
[22] X. Liu, J. Fei, A. Wang, W. Cui, P. Zhu, J. Li, *Angew. Chem., Int. Ed.* **2017**, *56*, 2660.
[23] T. Yuan, Y. Xu, J. Fei, H. Xue, X. Li, C. Wang, G. Fytas, J. Li, *Angew. Chem.* **2019**, *131*, 11189.
[24] H. C. Chang, C. Lu, C. L. Liu, W. C. Chen, *Adv. Mater.* **2015**, *27*, 27.
[25] S. K. Park, J. H. Kim, S. Y. Park, *Adv. Mater.* **2018**, *30*, 1704759.
[26] Z. Lü, X. Li, Y. Wang, J. Xiao, P. Xu, *Curr. Appl. Phys.* **2014**, *14*, 1465.
[27] R. Charvet, S. Acharya, J. P. Hill, M. Akada, M. Liao, S. Seki, Y. Honsho, A. Saeki, K. Ariga, *J. Am. Chem. Soc.* **2009**, *131*, 18030.
[28] A. Insuasty, C. Atienza, J. Luis López, J. Marco-Martínez, S. Casado, A. Saha, D. M. Guldi, N. Martín, *Sci. Rep.* **2015**, *5*, 14154.
[29] W. S. Li, Y. Yamamoto, T. Fukushima, A. Saeki, S. Seki, S. Tagawa, H. Masunaga, S. Sasaki, M. Takata, T. Aida, *J. Am. Chem. Soc.* **2008**, *130*, 8886.
[30] J. López-Andarias, J. L. López, C. Atienza, F. G. Brunetti, C. Romero-Nieto, D. M. Guldi, N. Martín, *Nat. Commun.* **2014**, *5*, 3763.
[31] M. Sathish, K. Miyazawa, J. P. Hill, K. Ariga, *J. Am. Chem. Soc.* **2009**, *131*, 6372.
[32] S. S. Babu, H. Möhwald, T. Nakanishi, *Chem. Soc. Rev.* **2010**, *39*, 4021.
[33] T. Michinobu, T. Nakanishi, J. P. Hill, M. Funahashi, K. Ariga, *J. Am. Chem. Soc.* **2006**, *128*, 10384.
[34] L. K. Shrestha, Q. Ji, T. Mori, K. Miyazawa, Y. Yamauchi, J. P. Hill, K. Ariga, *Chem. - Asian J.* **2013**, *8*, 1662.
[35] D. Bonifazi, O. Enger, F. Diederich, *Chem. Soc. Rev.* **2007**, *36*, 390.
[36] Y. Yamamoto, G. Zhang, W. Jin, T. Fukushima, N. Ishii, A. Saeki, S. Seki, S. Tagawa, T. Minari, K. Tsukagoshi, T. Aida, *Proc. Natl. Acad. Sci. U. S. A.* **2009**, *106*, 21051.
[37] M. H. Nurmawati, P. K. Ajikumar, R. Renu, C. H. Sow, S. Valiyaveettil, *ACS Nano* **2008**, *2*, 1429.
[38] M. J. Hollamby, M. Karny, P. H. H. Bomans, N. A. J. M. Sommerdjik, A. Saeki, S. Seki, H. Minamikawa, I. Grillo, B. R. Pauw, P. Brown, J. Eastoe, H. Möhwald, T. Nakanishi, *Nat. Chem.* **2014**, *6*, 690.
[39] V. S. Nair, Y. Pareek, V. Karunakaran, M. Ravikanth, A. Ajayaghosh, *Phys. Chem. Chem. Phys.* **2014**, *16*, 10149.
[40] J. L. Segura, N. Martín, D. M. Guldi, *Chem. Soc. Rev.* **2005**, *34*, 31.
[41] S. S. Babu, V. K. Praveen, A. Ajayaghosh, *Chem. Rev.* **2014**, *114*, 1973.
[42] P. Xue, P. Wang, B. Yao, J. Sun, P. Gong, Z. Zhang, C. Qian, R. Lu, *ACS Appl. Mater. Interfaces* **2014**, *6*, 21426.
[43] C. Zhang, J. Wang, J. J. Wang, M. Li, X. L. Yang, H. B. Xu, *Chem. - Eur. J.* **2012**, *18*, 14954.
[44] P. Xue, R. Lu, L. Zhao, D. Xu, X. Zhang, K. Li, Z. Song, X. Yang, M. Takafuji, H. Ihara, *Langmuir* **2010**, *26*, 6669.
[45] X. Yang, G. Zhang, D. Zhang, D. Zhu, *Langmuir* **2010**, *26*, 11720.
[46] S. K. Samanta, K. S. Subrahmanyam, S. Bhattacharya, C. N. R. Rao, *Chem. - Eur. J.* **2012**, *18*, 2890.
[47] V. S. Nair, R. D. Mukhopadhyay, A. Saeki, S. Seki, A. Ajayaghosh, *Sci. Adv.* **2016**, *2*, e1600142.
[48] K. Liu, S. Gao, Z. Zheng, X. Deng, S. Mukherjee, S. Wang, H. Xu, J. Wang, J. Liu, T. Zhai, Y. Fang, *Adv. Mater.* **2019**, *31*, 1808254.
[49] C. Yan, D. J. Pochan, *Chem. Soc. Rev.* **2010**, *39*, 3528.
[50] P. C. Dastoor, C. R. McNeill, H. Frohne, C. J. Foster, B. Dean, C. J. Fell, W. J. Belcher, W. M. Campbell, D. L. Officer, I. M. Blake, P. Thordarson, M. J. Crossley, N. S. Hush, J. R. Reimers, *J. Phys. Chem. C* **2007**, *111*, 15415.
[51] S. Das, P. Chakraborty, A. Shit, S. Mondal, A. K. Nandi, *J. Mater. Chem. A* **2016**, *4*, 4194.